Available online at www.sciencedirect.com

SCIENCE DIRECT

Biochimica et Biophysica Acta 1665 (2004) 65–74

BIOCHIMICA ET BIOPHYSICA ACTA BBA

http://www.elsevier.com/locate/bba

Reduced kinetic models of facilitative transport

Julio A. Hernández*, Juan Carlos Valle Lisboa

Sección Biofísica, Facultad de Ciencias, Universidad de la República, Iguá s/n esq. Mataojo, 11400 Montevideo, Uruguay

Received 14 May 2004; received in revised form 27 June 2004; accepted 28 June 2004
Available online 23 July 2004

Abstract

In spite of the highly complex structural dynamics of globular proteins, the processes mediated by them can usually be described in terms of relatively simple kinetic diagrams. How do complex proteins, characterized by undergoing transitions among a possibly very large number of intermediate states, exhibit functional properties that can be interpreted in terms of kinetic diagrams consisting of only a small number of states? One possible way of explaining this apparent contradiction is that, under some conditions, a reduction of the actual complete kinetic diagram that describes all of the macromolecular states and transitions takes place. In this work, we contribute with a formal basis to this interpretation, by generalizing the procedure of diagram reduction to the case of multicyclic kinetic diagrams. As an example, we apply the procedure to a complex kinetic model of facilitative transport. We develop Monte Carlo simulations to obtain the kinetic parameters of the complex model and we compare them with the ones analytically obtained from the reduced model. We confirm that, under some conditions, the kinetic behavior of the complex transporter is indistinguishable from the one of a four-state simple carrier model, derived from the former by diagram reduction. Besides introducing some novel methodological aspects, this work further contributes to the idea that, under many physiological and experimental conditions, a reduction occurs of the complete kinetic diagram that describes the dynamics of a globular protein.

Keywords: Facilitative transport; Kinetic model; Carrier; Diagram reduction

1. Introduction

Most functional properties of enzymes and membrane transport proteins are described by employing kinetic diagrams [1]. These diagrams consist of intermediate states of the macromolecule and transitions connecting these states. Although globular proteins exhibit complex structural dynamics, the catalytic and transport processes mediated by them are usually represented by relatively simple kinetic diagrams [1–4]. The analysis of this type of diagrams permits to derive expressions that, to a large extent, represent good approximations to interpret the available experimental evidence. The contemporary conception about the structure of macromolecules is markedly different from the one emerging from these simple descriptions of their kinetic properties. Findings obtained from the employment of diverse physical methods as well as the computational simulations of molecular dynamics suggest that, in the temperature range of most biological processes, globular proteins experience conformational transitions among a very large number of intermediate states [5–7]. Some evidence about gating kinetics in ionic channels also contributes to this idea [8]. In this way, two apparently contradictory conceptions have emerged: one that considers that only a small number of states should be taken into account in order to describe functional properties of enzymes and transport proteins and another that concludes that globular proteins are continuously experiencing transitions among a significantly larger number of structural states. How can these two conceptions be reconciled? One present view, which emerges from dynamic considerations, is that the functional performances of a protein can be interpreted by assuming the existence of hierarchical levels among the states of the macromolecule [7]. This idea has its kinetic counterpart in the conception that the kinetic schemes developed to

* Corresponding author. Fax: +5982 525 8629.
E-mail address: jahern@fcien.edu.uy (J.A. Hernández).

0005-2736/$ - see front matter © 2004 Elsevier B.V. All rights reserved.
doi:10.1016/j.bbamem.2004.06.015

represent biochemical and biophysical systems are condensed versions of the actual underlying mechanisms. This latter conception has somehow been present in diverse previous considerations that affirm, implicitly or explicitly, that the recognition of intermediate states of a macromolecule is determined by the time resolution and sensitivity of the experimental techniques, and that hidden states can be further revealed by the employment of more refined procedures [1,6,9–11]. The basic purpose of the present work is to provide a formal general kinetic basis to support this conception. Although the formalism developed here can find application to interpret experimental evidence in a wide variety of protein-mediated processes, we consider particularly the case of facilitative transport mediated by integral membrane proteins.

It has classically been accepted that the facilitative transport of ligands across biological membranes occurs via one of two distinctive elementary mechanisms: channel or carrier [3,12,13]. The essential difference between these two mechanisms is that while a single empty state of a channel is capable of binding a ligand from any of the two compartments separated by the membrane, a carrier offers at least two empty states to the ligand, each one available from one of the compartments only. The kinetic analysis of the net fluxes under initial conditions, a traditional method of classical enzymology [2,4], does not permit to distinguish between the two mechanisms. To do so, it is necessary to perform more involved kinetic studies, which require detailed analysis of the unidirectional fluxes. These studies provide a strict criteria to decide which particular permeation mechanism operates in a specific experimental situation [9,10]. In previous work [14], we showed that the kinetic carrier behavior could be exhibited by a wide variety of facilitative transport models, from the classical three- or four-state simple carrier model [3,12,13], to significantly more complex kinetic descriptions. This finding suggests one alternative to reconcile the two conceptions commented above, at least in the domain of transport proteins: some kinetic properties may be shared by very different transport systems, which range from very simple to significantly complex, from the point of view of the kinetic description of the mediated processes. As mentioned above, a more general alternative to interpret the finding of simple kinetic behaviors in complex protein-mediated processes is that the available experimental procedures only permit to obtain condensed or "reduced" versions of the complete diagram. The basic formal aspects of the procedures of diagram reduction have been developed by Hill [1] and have been utilized, for instance, to derive kinetic properties of electrogenic enzymes [15], to analyze the permeability properties of single-file water channels [16] and to reveal approximate channel-like behaviors of some carrier models [17]. The main objective of the present work is to generalize the procedure of diagram reduction to multicyclic kinetic diagrams, for the case that some of the states of the macromolecule are transient intermediates, and to propose it as a formal alternative to understand the relation between the relatively simple kinetic diagrams derived from the experimental studies and the complex mechanistic descriptions that may represent the detailed macromolecular processes. For illustrative purposes, we apply the method to the case of a complex model of facilitative transport. Under particular conditions, this complex model can be reduced to a simple carrier model. Therefore, under these conditions, the kinetic behavior of the original non-reduced model can be described in terms of the reduced model. We exemplify this situation by performing Monte Carlo simulations of the non-reduced model to obtain numerical values for its relevant experimental parameters and to confirm that, in some cases, this model can be strictly replaced by a four-state simple carrier model, obtained from the former by the procedure of diagram reduction. Besides the methodological aspects, this study also contributes to the concept that, under many physiological and experimental conditions, a natural reduction of the complete kinetic diagram that describes all the transitions of a globular protein takes place, thus yielding a phenomenological behavior that can be represented in terms of a simpler kinetic description.

2. Results and discussion

2.1. Reduction of a complex model of facilitative transport to a simple carrier model

A possible mechanism of facilitative transport of a ligand across a biological membrane, mediated by an integral protein, is shown in Fig. 1A. Although not extraordinarily involved, this mechanism is nevertheless significantly more complex than the one represented by the classical four-state simple carrier model (SCM, see Fig. 3 below). In this latter case, the transporter pre-exists in only two conformational states, each one capable of binding the ligand from only one of the compartments separated by the membrane. For the case of the model shown in Fig. 1A, the transporter transits among a larger number of unoccupied states than the SCM (six). Still more complex situations can easily be conceived, where the transporter undergoes structural transitions between tens or even hundreds of free states, only two of which being able to bind the ligand with a high affinity (i.e., recognizable by experimental procedures). Fig. 1B shows the state diagram corresponding to the mechanistic model in Fig. 1A. This diagram results extremely complex for any analytical purpose. Indeed, in terms of the graphical algorithm [1] the diagram depicted in Fig. 1B contains seven cycles (Fig. 2) and generates more than 2000 directional diagrams. The model in Fig. 1 thus exemplifies a typical situation in biology, where a high degree of analytical complexity is already achieved at supposedly not-so-complicated models, at least from the point of view of their biological feasibility. Anyway, we adopt here the

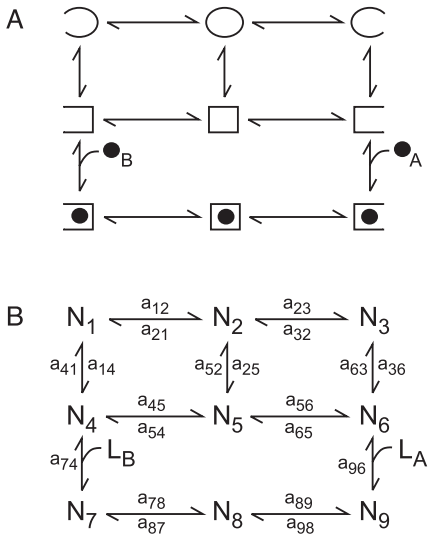

Fig. 1. A complex facilitative membrane transporter that mediates the translocation of a ligand (L) between compartments A and B. (1A) Scheme showing the mechanistic aspects of the macromolecular transitions (black circles: L). Only two of the conformational states of the transporter are capable of binding L from A or B. (1B) The corresponding state diagram. $N_1,\ldots, N_9$ are the intermediate states of the macromolecule. L_A and L_B represent the ligand, binding from compartments A and B, respectively. The a's represent rate constants, governing the corresponding transitions.

model in Fig. 1 as an example to illustrate the methods utilized in this work and study its kinetic behavior not via its explicit analysis but by performing Monte Carlo simulations. We employ this methodology below to confirm that, under the appropriate conditions, the kinetic behavior of the model in Fig. 1B is similar to that of a four-state SCM, obtained from the former by diagram reduction.

The reduction of the diagram shown in Fig. 1B to a four-state diagram can be achieved if, for instance, states N_1, N_2, N_3, N_5 and N_8 are transient intermediates [1,16,17]. The resulting reduced model is shown in Fig. 3. As can be seen, this model corresponds to the classical SCM [3,12,13]. The reduction is performed in Appendix A. In particular, we introduce there the generalization of the method of diagram reduction to multicyclic diagrams and obtain explicit expressions for the reduced rate constants r_{46}, r_{64}, r_{79} and r_{97} (Fig. 3) in terms of the original ones. Fig. 4 shows the diagrammatic interpretations of r_{46} and r_{64}. As a reference for this work, we summarize in Appendix B the kinetic characterization of carriers, in terms of the analysis performed by Lieb and Stein [10]. There, we also show the explicit expressions for the relevant experimental parameters for the particular case of the SCM (Fig. 3).

The reduction of the model depicted in Fig. 1B to yield the four-state model in Fig. 3 represents one particular case in which the non-reduced macromolecular states belonging to the region of ligand-free states exactly correspond with the ones capable of binding the ligand. Other diverse situations are certainly conceivable, where such coincidence does not take place. In addition, a kinetic model can also be reduced if a rapid equilibrium exists between some neighboring states [1,17]. In fact, the identification of a particular intermediate state is a consequence of the time scale of the experimental procedure employed. Hence, a "state" may actually correspond to a number of non-identifiable sub-states in rapid equilibrium between them [1]. A mixed situation may occur, where the diagram reduction takes place as a consequence of the existence of both transient intermediate states and rapid equilibrium between some neighboring states. As mentioned, in view of the illustrative character of this study, we only consider here the case of the model reduction that generates the diagram in Fig. 3. Finally, it is important to emphasize here that the reduction procedure does not imply any modification of the fundamental mechanism of action of the protein [17]. That is, for the case of the diagram depicted in Fig. 1B, its reduction to the one shown in Fig. 3 can only be considered to be the application of a particular technique to reveal an approximate kinetic behavior under specific conditions and not a transformation of a molecular mechanism into another. For both kinetic diagrams, the underlying molecular mechanism corresponds to the one shown in Fig. 1A.

In principle, although previous evidence suggests that the complex transporter model represented in Fig. 1B should exhibit elementary carrier-like kinetic behavior [14], at present there is no a priori demonstration to strictly support that idea. In this respect, it must be emphasized that the objective of this work is not to reveal the existence of a carrier-like behavior of the complex model depicted in Fig. 1B in general, but to find conditions where its behavior is indistinguishable from that of a four-state simple carrier model, both in the stationary and time-dependent situations (Appendix A). The reduced model (Fig. 3) satisfies the conditions required by the "general carrier model" [14], therefore a simple carrier-like kinetic behavior is to be expected for it. This obviously implies that, under the reduction conditions, the full original model in Fig. 1B will also exhibit a similar carrier-like kinetic behavior, as confirmed by the Monte Carlo simulations performed below. The reduction of intermediate empty states of the carrier (e.g., states N_1, N_2, N_3, N_4, N_5 and N_6 of the model in Fig. 1B) may affect the original kinetic behavior of the transport system by modifying the general forms of the expressions representing the unidirectional fluxes. An example of this is the appearance of channel-like kinetic behaviors in well-defined carrier systems when the isomerization transition between the two empty forms of the carrier can be reduced [13,17]. This finding contributes to conceive that, at least in the realm of transport processes, some model reductions may significantly affect the original characteristic kinetics. For the particular case of the model shown in Fig. 1B this would imply that other reduced models, obtained from it by discarding at least one of the intermediate empty states of the transporter capable of binding the ligand, may not exhibit similar characteristic transport kinetics to it. On the other hand, in general it is not expected that the reduction of ligand–transporter complexes belonging to a

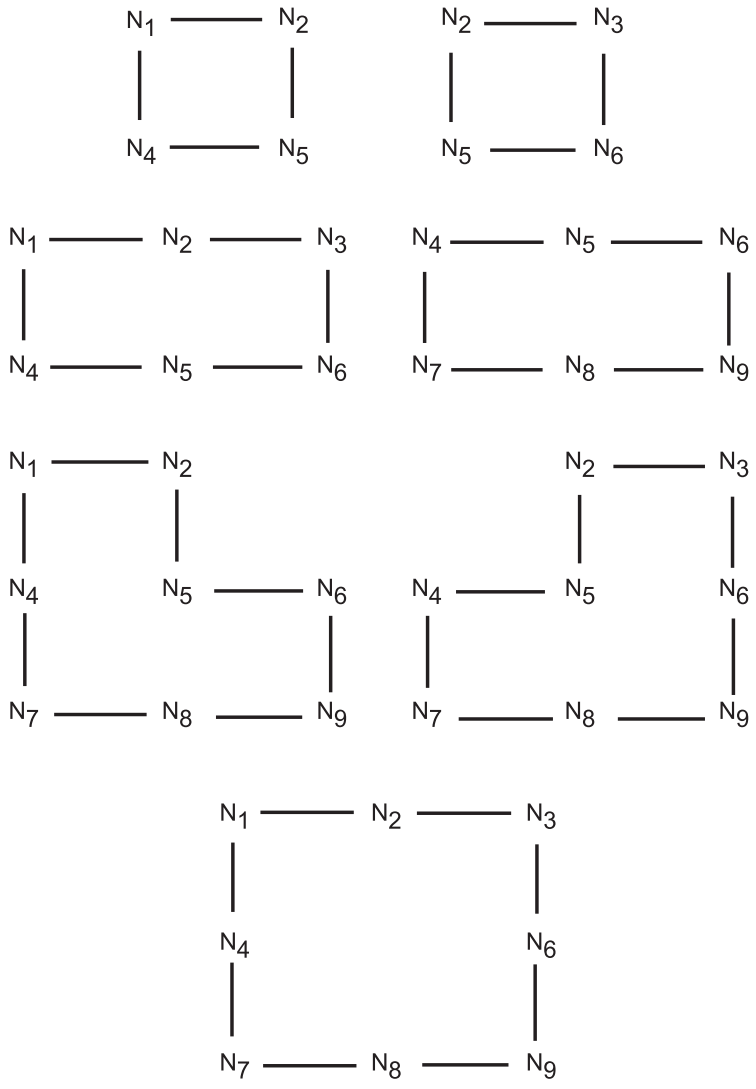

Fig. 2. Cycles contained in the state diagram shown in Fig. 1B.

linear path (e.g., state N_8 of the model in Fig. 1B) would affect the general steady-state kinetic properties of the system [10,11,13]. Therefore, reduced models obtained by discarding this class of states from the diagram will not modify the original type of characteristic transport kinetics.

2.2. Monte Carlo simulations of the complex transporter model

Under the conditions given by Eq. (A2) the kinetic behavior of the original model shown in Fig. 1B can be described in terms of the model in Fig. 3, both for the time-dependent and steady-state situations. In order to illustrate that the two kinetic models exhibit, in that case, similar kinetic properties, we performed Monte Carlo simulations of the original model (Fig. 1B) and compared the results with those obtained from the explicit study of the model in Fig. 3. As mentioned above, the fundamental reason for the employment of Monte Carlo methods is that the derivation of explicit equations for the unidirectional fluxes for the case of the full model in Fig. 1B represents a cumbersome task. The procedures utilized in this section are outlined in Appendix C.

Fig. 5 resumes some results obtained from Monte Carlo simulations of the model in Fig. 1B and their comparison with the ones calculated employing the explicit expressions corresponding to the reduced SCM in Fig. 3, for a symmetric pattern of the numerical values of the rate constants (see the legend in Fig. 5). The figure reveals that, as predicted (Appendix A), the kinetic behavior of the original model approaches the one of the reduced model when the numerical values of the rate constants tend to satisfy relation (A2). Not explicitly shown in Fig. 5 is the finding that, as suggested from a previous study [14], the numerical results obtained for the relevant kinetic parameters (K, R_{00}, R_{AB}, R_{BA} and R_{ee}) from the simulations of the model in Fig. 1B satisfy Eq. (A11), both under reducing and non-reducing conditions. In other words, the simulations show that in its full form, this model already exhibits the carrier-like kinetic behavior (Appendix B). The symmetric character of the

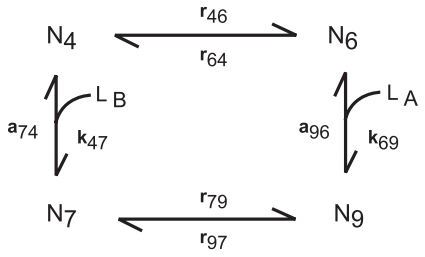

Fig. 3. Reduced state diagram obtained from the original diagram shown in Fig. 1B by assuming that states N_1, N_2, N_3, N_5 and N_8 are transient intermediates. The a's and k's are original rate constants, the r's are reduced rate constants.

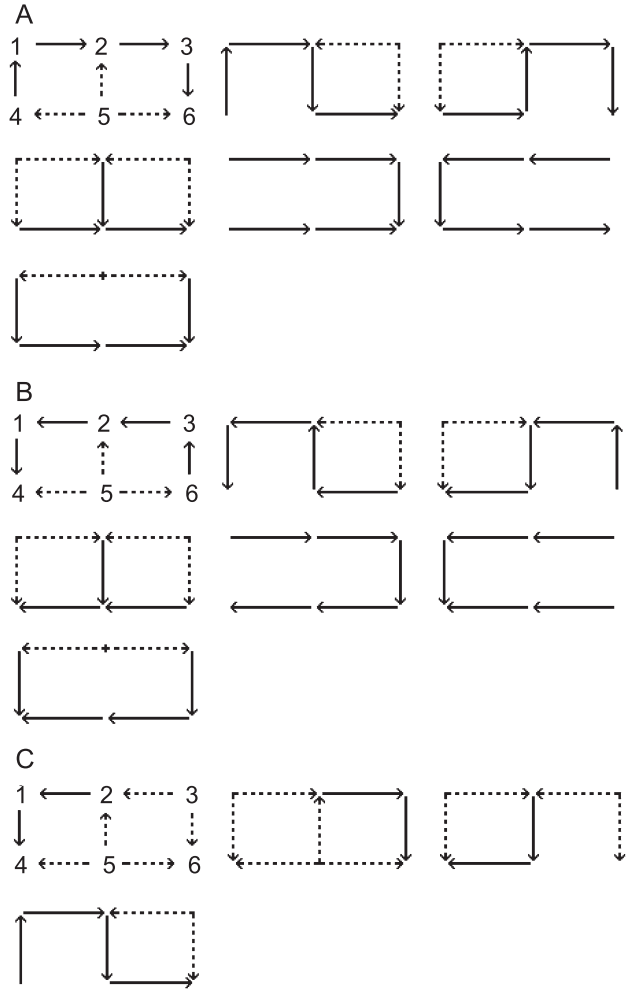

Fig. 4. Diagrammatic representation of the numerator of r_{46} (4A), numerator of r_{64} (4B) and denominator of r_{46} and r_{64} (4C) (Eq. (A8b)). As a reference, some schemes show the subscripts of the corresponding states. Each solid and broken arrow corresponds to a rate constant. In order to minimize the figure size, some of the schemes represent several terms. In these schemes, more than one broken arrow emerge from some of the states. To obtain each term (a product of rate constants), only one broken arrow should be included per each one of these states. Thus, for instance, the scheme depicting the state subscripts in 4C represents the six terms contained in the expression:

$$a_{21}a_{14}(a_{32}+a_{36})(a_{52}+a_{54}+a_{56}).$$

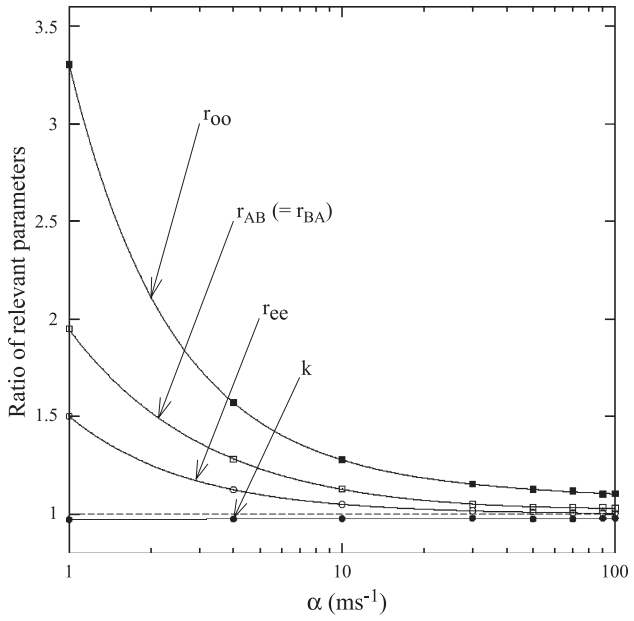

Fig. 5. Comparison between the kinetic properties of the complete model in Fig. 1B and the ones of the reduced model in Fig. 3, for a symmetric pattern of the numerical values of the rate constants. For this case, we assumed that $a_{14}=a_{36}=a_{54}=a_{56}=a_{87}=a_{89}\equiv\alpha$. For the two models, in order to perform the numerical calculations, these rate constants have been replaced by the variable α in the corresponding expressions. The plot shows the ratios of the Monte Carlo-estimated kinetic parameters (model in Fig. 1B) to the theoretically calculated ones for the reduced transporter (model in Fig. 3), as functions of α (ms^{-1}). All the other constants were set equal to 1.0 (ms^{-1} or $mM^{-1}\,ms^{-1}$). The relevant parameters (R_{ie}, R_{ei}, R_{oo}, R_{ee}, K) of the Monte Carlo-simulated model in Fig. 1B were obtained as described in Appendix C. Each point in the graph is determined from the result of 5000 simulations. Standard errors were always less than 1% and are not displayed in the graph. The theoretical parameters of the SCM shown in Fig. 3 were obtained employing Eq. (A13), with the reduced rate constants given by Eqs. (A8b) and (A9). The ratios are defined as follows: $r_{oo}=R_{oo}$ (full model)/R_{oo} (SCM); $r_{ee}=R_{ee}$ (full model)/R_{ee}(SCM); $r_{BA}=R_{BA}$ (full model)/R_{BA} (SCM); $r_{AB}=R_{AB}$ (full model)/R_{AB}(SCM); $k=K$ (full model)/K (SCM).

numerical values chosen for the rate constants underlies the obtainment of equal values for the parameters R_{AB} and R_{BA}, both for the numerical simulations of the original non-reduced model and for the explicit calculations of the reduced SCM. The results from the study of non-symmetrical cases are shown in Table 1. It can be seen in this table that, analogously to the symmetrical situation, the accomplishment of relation (A2) also determines that, as expected, the original model and the reduced SCM are both characterized by the same kinetic parameters (case "b").

To be noted, for the case of the original complete model the parameters K, R_{00}, R_{AB}, R_{BA} and R_{ee} represent the best fits to the simulation results. However, for the case of the reduced SCM, the numerical values for the corresponding parameters are calculated from analytical equations; therefore they do not introduce any error to the ratios shown in Fig. 5. For the Monte Carlo experiments, the parameters R_{00}, R_{AB}, R_{BA} and R_{ee} can be directly derived from the maximal velocities, but the parameter K is derived from half-saturation constants utilizing any of the predetermined Rs (Eq. (A12)).

Table 1
Monte Carlo simulations of the model in Fig. 1B for non-symmetrical cases

	R_{AB} (mM^{-1} ms)	R_{BA} (mM^{-1} ms)	R_{oo} (mM^{-1} ms)	R_{ee} (mM^{-1} ms)	K (mM)
(a) Theoretical	10.89	6.06	4.44	12.50	2.81
(a) Monte Carlo	13.99	9.01	8.18	15.05	2.78
(b) Theoretical	11.25	7.49	6.23	12.50	2.01
(b) Monte Carlo	11.24	7.52	6.53	12.48	1.98

The kinetic constants equal 1 (ms^{-1} or mM^{-1} ms^{-1}), except for: (a) $a_{14}=a_{54}=a_{87}=4$ ms^{-1}; (b) $a_{14}=a_{54}=a_{87}=1000$ ms^{-1}; $a_{36}=a_{56}=a_{89}=250$ ms^{-1}. With these parameters, the resulting relevant parameters are characteristic of an asymmetric transporter [13]. In this table, "Theoretical" refers to the parameters obtained for the SCM (Fig 3), calculated employing Eqs. (A8b), (A9) and (A13). The number of repetitions for each point was 5000, which determined that the standard error was significantly lower than 1%.

As a consequence, the uncertainty associated with K is higher than the uncertainty of the other parameters. In any case, significantly low values of the standard errors were obtained for all the parameters (see Fig. 5).

Besides constituting a relevant methodological tool per se, the Monte Carlo simulations included in this study have been developed with the purpose of illustrating the validity of the reduction process with a particular example. In this latter respect, the importance of the simulations should basically not be considered to be to prove the validity of the reduction procedure, but to show the range of parameter values for which the full model is indistinguishable from a simple four-state carrier model. It must be remarked that the steady-state measurements do not suffice to distinguish between a complex model, like the one shown in Fig. 1B, and a simple carrier model. The reason for this is that, as commented above, the simulations show that the full model already exhibits steady-state kinetic properties that can be fitted with phenomenological SCM equations (Appendix A). In relation with this it must be realized that, for the case of carrier-mediated transport, there are more degrees of freedom for choosing kinetic constants than experimentally determined parameters. Thus, a particular set of relevant experimental parameters may be interpreted in terms of a myriad of different models satisfying carrier kinetics, ranging from three-state to extremely complex models [13,14]. In contrast, as also mentioned above, a single reduced model strictly replaces an original complex one for the description of both the steady-state and time-dependent situations (Appendix A), for a particular set of values of the rate constants satisfying the reduction conditions.

3. Conclusions

In this essentially methodological work we have extended the procedure of diagram reduction to the case of multicyclic diagrams. In particular, we have employed the procedure to derive a reduced four-state simple carrier model from a significantly more complex transporter model. We have thus contributed to the previously discussed concept [17] that approximate behaviors of diverse kinetic models of facilitative transport can be uncovered in a straightforward manner by applying the reduction technique. We have also introduced a Monte Carlo procedure designed to derive characteristic kinetic parameters from the stochastic simulations of a complex transporter model. The results of these simulations were used here to illustrate that, in effect, under particular conditions, the reduced model exhibits a kinetic behavior indistinguishable from the one of the original model. Although the simulation procedures employed here have only considered steady-state properties, the reduced model obtained is kinetically equivalent to the original complex one in every point of the time domain. The simulations also permitted us to confirm that, as suggested from previous studies [14], a transporter characterized by a relatively complex kinetic design, like the one shown in Fig. 1B, nevertheless may exhibit the typical kinetic behavior of a simple carrier.

The main contribution of this work has therefore been to provide with a simple, straightforward general formalism as an alternative to understand the finding of simple kinetic behaviors in complex protein-mediated processes. In this way, the results of this study contribute to the idea that, in general, the particular kinetic diagram designed to describe the experimental findings about the functional properties of a protein could actually be a condensed or reduced diagram. That is, although the basic mechanism of operation of the macromolecule may correspond to a complex state diagram, the researcher is able to recognize only some states and transitions. These states and transitions conform a reduced model, which is basically a consequence of the time scale of the experimental methodology employed. Essentially, this idea may have a counterpart in the hierarchical organization of the energy landscapes proposed by some authors in order to interpret the performance of specific biochemical properties by proteins fluctuating among many conformational states [7]. From the perspective of the kinetic formalism, the concept of diagram reduction may provide with an alternative way to understand why dynamically complex macromolecules perform functions describable in terms of simple models.

Acknowledgments

Supported by grants from the Comisión Sectorial de Investigación Científica (C.S.I.C.) de la Universidad de la República, and by the Programa para el Desarrollo de las Ciencias Básicas (PEDECIBA), Uruguay.

Appendix A. Reduction of a multicyclic kinetic diagram

We introduce here a procedure to obtain a reduced model from a multicyclic kinetic diagram, for the case that some states are transient intermediates. The method described in this section represents an extension of the one proposed by Hill [1] for the reduction of linear sequences of transitions. Instead of deriving general expressions, the procedure is developed employing the diagram shown in Fig. 1B as an example. The method introduced here can be adapted in a straightforward manner to handle more complicated kinetic schemes.

The diagram shown in Fig. 1B can be reduced to a four-state one if, for instance, states N_1, N_2, N_3, N_5 and N_8 are transient intermediates [1,17] (Fig. 3). Under these conditions

$$p_1, p_2, p_3, p_5, p_8 \ll p_4, p_6, p_7, p_9, \tag{A1}$$

where p_i (i=1, 2,..., 9) is the probability (frequency) of the ith state in the complete ensemble. For the example under consideration, relation (A1) is fulfilled if

$$a_{14}, a_{54}, a_{36}, a_{56} \gg a_{12}, a_{21}, a_{23}, a_{32}, a_{25}, a_{52} \text{ and } a_{87}, a_{89} \gg a_{78}, a_{98}. \tag{A2}$$

From Eq. (A1) it can be assumed that

$$dN_j/dt = 0, \tag{A3}$$

where j=1, 2, 3, 5, 8 (transient states) and where N_j now represents the membrane density (expressed, for instance, in mol cm^{-2}) of the jth state of the transporter.

The reduction procedure can proceed by independently reducing the multicyclic network of transitions contained between states N_4 and N_6 and the linear path contained between states N_7 and N_9. For the case of the multicyclic portion of the diagram defined by considering states N_1,...,N_6 only, we may write, from Eq. (A3),

$$\mathbf{R}\ N_{\mathrm{R}} = B, \tag{A4}$$

where $\mathbf{R}$ is the "reduction matrix" and N_{R} and B are column vectors, given by

$$\mathbf{R} = \begin{bmatrix} -(a_{12}+a_{14}) & a_{21} & 0 & 0 \\ a_{12} & -(a_{21}+a_{23}+a_{25}) & a_{32} & a_{52} \\ 0 & a_{23} & -(a_{32}+a_{36}) & 0 \\ 0 & a_{25} & 0 & (a_{52}+a_{54}+a_{56}) \end{bmatrix}$$

$$N_R = \begin{bmatrix} N_1 \\ N_2 \\ N_3 \\ N_5 \end{bmatrix}, \text{ and } B = \begin{bmatrix} -a_{41}\ N_4 \\ 0 \\ -a_{63}\ N_6 \\ -(a_{45}\ N_4 + a_{65}\ N_6) \end{bmatrix}. \tag{A5}$$

Similarly to the reduced states, in Eq. (A5) N_4 and N_6 represent the membrane densities of the corresponding states.

The solution of Eq. (A4) yields expressions for N_1, N_2, N_3, and N_5 as functions of N_4, N_6 and the rate constants:

$$N_1 = \det \mathbf{R}_1/\det \mathbf{R}, \ldots, N_5 = \det \mathbf{R}_5/\det \mathbf{R}, \tag{A6}$$

where det $\mathbf{X}$ is the determinant of $\mathbf{X}$ and where the matrices $\mathbf{R}_1$, $\mathbf{R}_2$, $\mathbf{R}_3$ and $\mathbf{R}_5$ are obtained from $\mathbf{R}$ by replacing the first, second, third and fourth columns by B, respectively.

The rate equations for states N_4 are N_6 are given by

$$\mathrm{d}N_4/\mathrm{d}t = a_{14}N_1 - (a_{42}+a_{45})N_4 + a_{54}N_5$$

$$\mathrm{d}N_6/\mathrm{d}t = a_{36}N_3 + a_{56}N_5 - (a_{63}+a_{65})N_6. \tag{A7}$$

Under the reduction condition determined by Eq. (A2), N_1, N_3, and N_5 can be replaced by expression (A6). In this particular case, the rate equations for N_4 and N_6 become

$$\begin{aligned} \mathrm{d}N_4/\mathrm{d}t &= -r_{46}\ N_4 + r_{64}\ N_6 \\ \mathrm{d}N_6/\mathrm{d}t &= r_{46}\ N_4 - r_{64}\ N_6, \end{aligned} \tag{A8a}$$

where the reduced rate constants r_{46} and r_{64} (Fig. 3) are given by

$$r_{46} = (1/\det\mathbf{R})\{a_{41}a_{12}a_{23}a_{36}(a_{52}+a_{54}+a_{56}) + a_{41}a_{12}a_{25}a_{56}(a_{32}+a_{36}) + a_{45}a_{52}a_{23}a_{36}(a_{12}+a_{14}) + a_{45}a_{56}[a_{12}a_{25}(a_{32}+a_{36}) + a_{14}a_{36}(a_{21}+a_{23}) + a_{14}a_{25}(a_{32}+a_{36}) + a_{12}a_{23}a_{36} + a_{32}a_{21}a_{14}]\}$$

$$r_{64} = (1/\det\mathbf{R})\{a_{63}a_{32}a_{21}a_{14}(a_{52}+a_{54}+a_{56}) + a_{65}a_{52}a_{21}a_{14}(a_{32}+a_{36}) + a_{63}a_{32}a_{25}a_{54}(a_{12}+a_{14}) + a_{65}a_{54}[a_{12}a_{25}(a_{32}+a_{36}) + a_{14}a_{36}(a_{21}+a_{23}) + a_{14}a_{25}(a_{32}+a_{36}) + a_{12}a_{23}a_{36} + a_{32}a_{21}a_{14}]\} \quad \text{(A8b)}$$

Fig. 4 shows a diagrammatic version of the reduced rate constants r_{46} and r_{64}. Notice that the terms in the numerators of these reduced constants correspond to the paths connecting states N_4 and N_6 and their appendages.

Since state N_8 is contained in the linear path connecting states N_7 and N_9. the reduced rate constants r_{79} and r_{97} (Fig. 3) are simply given by [1,17]

$$r_{79} = a_{78}a_{89}/(a_{87}+a_{89})$$

$$r_{97} = a_{98}a_{87}/(a_{87}+a_{89}). \quad \text{(A9)}$$

Appendix B. Kinetic characterization of carriers

The kinetic characterization of channels and carriers has been performed by Lieb and Stein [9,10,13]. As a reference to the present work, we summarize here the basic kinetic properties of carriers, in terms of the proposal made by these authors.

The unidirectional ligand fluxes v_{AB} and v_{BA} (in the A→B and B→A directions, respectively), mediated by a carrier, are given by

$$v_{AB} = (K + L_B)L_A/D \text{ and } v_{BA} = (K + L_A)L_B/D, \quad \text{(A10a)}$$

with

$$D = K^2R_{00} + K\ R_{AB}L_A + K\ R_{BA}L_B + R_{ee}L_AL_B.$$

The net flux J_L (positive in the A→B direction) is given by

$$J_L = v_{AB} - v_{BA}. \quad \text{(A10b)}$$

In Eq. (A1), L_A and L_B are the ligand concentrations in compartments A and B, respectively, and K, R_{00}, R_{AB}, R_{BA} and R_{ee} are the relevant experimental parameters. The explicit expressions for these parameters depend on the particular model considered [13,14].

The thermodynamic restriction of detailed balance is employed to derive the following property, characteristic of carrier systems [10,13]:

$$R_{ee} + R_{00} = R_{AB} + R_{BA}. \quad \text{(A11)}$$

The maximum velocities (Vs) and half-saturation constants (Ks) characterizing the diverse flux determinations can be expressed in terms of the relevant experimental parameters [10,13]:

$$\begin{aligned}
&V^{zt}_{AB} = 1/R_{AB}; \quad K^{zt}_{AB} = K\ R_{00}/R_{AB};\\
&V^{zt}_{BA} = 1/R_{BA}; \quad K^{zt}_{BA} = K\ R_{00}/R_{BA};\\
&V^{it}_{AB} = 1/R_{ee}; \quad K^{it}_{AB} = K\ R_{BA}/R_{ee};\\
&V^{it}_{BA} = 1/R_{ee}; \quad K^{it}_{BA} = K\ R_{AB}/R_{ee};\\
&V^{ic}_{AB} = 1/R_{AB}; \quad K^{ic}_{AB} = K\ R_{AB}/R_{ee};\\
&V^{ic}_{BA} = 1/R_{BA}; \quad K^{ic}_{BA} = K\ R_{BA}/R_{ee};\\
&V^{ee} = 1/R_{ee}; \quad K^{ee} = K\ R_{00}/R_{ee}, \quad \text{(A12)}
\end{aligned}$$

where the particular experimental condition is indicated (zt: zero trans; it: infinite trans; ic: infinite cis; ee: equilibrium exchange). It must be noted that an unidirectional flux is considered to take place from the *cis* to the *trans* compartment.

The kinetic behavior of a particular carrier system can therefore be characterized by the specific values of the relevant experimental parameters K, R_{00}, R_{AB}, R_{BA} and R_{ee}. However, these parameters do not suffice to decide what particular molecular mechanism is at work [13,14]. For the specific case of the four-state simple carrier model, the explicit expressions for these parameters become, in terms of the rate constants employed in Fig. 3,

$$K = (r_{64}/k_{69}) + (r_{46}/k_{47}) + [a_{74}r_{46}/(k_{47}r_{79})]$$

$$NR_{AB} = (1/a_{74}) + (1/r_{46}) + (1/r_{97}) + [r_{79}/(r_{97}\ a_{74})]$$

$$NR_{BA} = (1/a_{96}) + (1/r_{64}) + (1/r_{79}) + [r_{97}/(r_{79}\ a_{96})]$$

$$NR_{ee} = (1/a_{74}) + (1/r_{97}) + [r_{79}/(r_{97}\ a_{74})] + (1/a_{96}) + (1/r_{79}) + [r_{97}/(r_{79}\ a_{96})]$$

$$NR_{00} = (1/r_{46}) + (1/r_{64}), \tag{A13}$$

where N is the total membrane density of the carrier.

Appendix C. Monte Carlo simulations and parameter determination

The simulation procedure utilized in this work is based on the direct method of Gillespie [18,19]. The main advantage of this algorithm is that the time step of the simulation is automatically and exactly selected (for a complete discussion of the properties of the algorithm and possible approximations, see Ref. [20]). Although the version used here was not optimized for computing load, it was chosen because of the relative ease of programming. We now describe the essential aspects of the methodology employed in this study.

At any time, including t=0, the system (a single macromolecule or a set of macromolecules) is in a particular state, chosen at random or as a predefined initial condition. For each state X there are several reacting channels to choose from, which can be numbered. Let μ be the index of possible reaction channels. With this notation, the relevant density function is:

$$P(\tau,\mu)d\tau = \text{Probability that given the stateX in time t, the next reaction occurs in the infinitesimal interval}(t+\tau, t+\tau+d\tau)\text{and is of type } \mu, \tag{A14}$$

where, as mentioned, μ =1, 2,... is the index of reactions available to state X and τ is the stochastic time step.

The probability density (A14) can be derived from the mass action law. If the available reaction channels are ζ=1, 2,..., μ,..., it reads [18,20]:

$$P(\tau,\mu) = a_\mu e^{-\sum_\zeta a_\zeta \tau}, \tag{A15}$$

where a_ζ represents the probability per unit time of the corresponding transition (i.e., the pseudo-first order rate constant). To implement the algorithm, a uniform random number in the interval (0, 1), r_1, is selected employing the routine RAN2 [21] and transformed using

$$\tau = \frac{1}{a_0}\ln\frac{1}{r_1}, \tag{A16}$$

where $a_0 = \sum_\zeta a_\zeta$. A second uniform random number, r_2, is used to decide which reaction is to occur given that the next reaction happens at time $t+\tau$. This requires to search for the μ that satisfies the following relation:

$$\sum_{\zeta=1}^{\mu-1} a_\zeta < r_2 a_0 \le \sum_{\zeta=1}^{\mu} a_\zeta. \tag{A17}$$

The procedure just described assures that each pair (μ, τ) is a realization of the density function defined by Eq. (A14).

In our particular case, we simulated a single macromolecular transporter as it followed the random walk among the available molecular states. Starting from a randomly chosen state, the simulation advanced as described above. After recording the new state and the time of the transition, the procedure was iterated up to a predefined total time. During each simulation the unidirectional fluxes from compartment A to B (B to A) (see Fig. 1B) were calculated as the number of instances that a ligand molecule was transported from A to B (B to A) divided by the total simulation time (after discarding the 100 initial transitions). To do so, for instance, we counted one event of transport in the direction A→B each time the transporter, starting from the state that binds the ligand at compartment A (N_4 in the model in Fig. 1B), effectively bound the ligand from A *and* released it to B, irrespectively of what happened in between. Simulations were performed for different values of ligand concentration, in order to obtain the relevant kinetic parameters R_{ie}, R_{ei}, R_{oo}, R_{ee}, K (Appendix B). For the estimation of these parameters, we simulated the usual experimental paradigms and fitted the suitable equations using GNUPLOT (freeware package available from ftp://ftp.gnuplot.info/pub/gnuplot/). Each simulation was repeated 5000 times, in order to obtain reliable estimates of the standard errors of those parameters.

References

[1] T.L. Hill, Free Energy, Free Energy Transduction in Biology, Academic Press, New York, 1977, pp. 1–32, 193–200.
[2] M. Dixon, E.C. Webb, Enzymes, 3rd edition, Academic Press, New York, 1979.
[3] O.S. Andersen, Kinetics of ion movement mediated by carriers and channels, Methods Enzymol. 171 (1989) 62–112.
[4] A. Cornish-Bowden, Fundamentals of Enzyme Kinetics, Portland Press, London, 1995, pp. 19–158.
[5] J.A. McCammon, S.C. Harvey, Dynamics of Proteins and Nucleic Acids, Cambridge University Press, New York, 1987.
[6] H. Guttfreund, Kinetics for the Life Sciences, Cambridge University Press, Cambridge, 1995, pp. 103–107, 248–261.
[7] H. Frauenfelder, Proteins: paradigms of complexity, Proc. Natl. Acad. Sci. U. S. A. 99 (2001) 2479–2480.
[8] J.B. Bassingthwaighte, L.S. Liebovitch, B.J. West, Fractal Physiology, Oxford University Press, New York, 1994, pp. 177–209.
[9] W.R. Lieb, W.D. Stein, Testing and characterizing the simple pore, Biochim. Biophys. Acta 373 (1974) 165–177.
[10] W.R. Lieb, W.D. Stein, Testing and characterizing the simple carrier, Biochim. Biophys. Acta 373 (1974) 178–196.
[11] I.H. Segel, Enzyme Kinetics, John Wiley and Sons, New York, 1975, pp. 534–543.
[12] S.G. Schultz, Basic Principles of Membrane Transport, Cambridge University Press, Cambridge, 1980, pp. 33–41, 85, 95–96.
[13] W.D. Stein, Transport and Diffusion across Cell Membranes, Academic Press, Orlando, Fl, 1986, pp. 158–257.
[14] J.A. Hernández, Simple carrier kinetics in complex membrane transporters, J. Membr. Biol. 165 (1998) 235–242.
[15] U.-P. Hansen, D. Gradmann, D. Sanders, C.L. Slayman, Interpretation of current–voltage relationships for "active" ion transport systems: I.

Steady-state reaction-kinetic analysis of class-I mechanisms, J. Membr. Biol. 63 (1981) 165–190.
[16] J.A. Hernández, J. Fischbarg, Kinetic analysis of water transport through a single-file pore, J. Gen. Physiol. 99 (1992) 645–662.
[17] J.A. Hernández, Open channel-like behavior of reduced carrier models, J. Membr. Biol. 180 (2001) 177–185.
[18] D.T. Gillespie, A general method for numerically simulating the stochastic time evolution of coupled chemical reactions, J. Comput. Phys. 22 (1976) 403–434.
[19] M.A. Gibson, J. Bruck, Efficient exact stochastic simulation of chemical systems with many channels, J. Phys. Chem. 104 (2000) 1876–1889.
[20] D.T. Gillespie, Approxímate accelerated stochastic simulation of chemically reacting systems, J. Chem. Phys. 115 (2001) 1716–1733.
[21] W.H. Press, S.A. Teukolsky, W.T. Vetterling, B.P. Flannery, Numerical Recipes in C: the Art of Scientific Computing, Cambridge University Press, Cambridge, 1995, pp. 278–282.